

Fuzzy-Set Theoretic Control Design for Aircraft Engine Hardware-in-the-Loop Testing: Mismatched Uncertainty and Optimality

Muxuan Pan , Yun Xu, Binbin Gu, Jinquan Huang, and Ye-Hwa Chen 

Abstract—A novel robust control design is proposed for aircraft engines. The engine is modeled as an uncertain dynamic system, whose uncertainty may be (possibly fast) time-varying. The possible value of the uncertainty is prescribed to be within fuzzy sets. This distinguishes our modeling from the Takagi–Sugeno inference system. The uncertainty is divided into matched and mismatched portions. While the matched uncertainty lies within the range space of the input matrix, the mismatched uncertainty falls outside, which poses a significant challenge for the control design. The objective is to propose a new robust control design for aircraft engines, which are subject to mismatched uncertainty. A robust control, which is deterministic and is not IF–THEN fuzzy rule-based, is designed. The control design parameter needs to be feasible, i.e., within a prescribed range. Some prescribed deterministic performances of the system are guaranteed. By taking the control cost and the performance threshold into consideration, which is under the influence of both matched and mismatched uncertainty, the unique optimal choice of the design parameter is proposed. As a result, this control design delicately blends optimality with mismatched uncertainty. This design is applied to a turbofan engine. Hardware-in-the-loop laboratory testing in the flight envelope demonstrates the superiority of the control design.

Index Terms—Aircraft engine, fuzzy system, hardware-in-the-loop testing, mismatched uncertainty, optimal design, robust control.

I. INTRODUCTION

AIRCRAFT engines play an important role in both civil and military applications [1]. At present, with increasing

Manuscript received November 5, 2020; revised March 24, 2021 and May 13, 2021; accepted June 22, 2021. Date of publication July 14, 2021; date of current version February 9, 2022. This work was supported in part by the National Science and Technology Major Project under Grant 2017-V-0004-0054. (Corresponding author: Muxuan Pan.)

Muxuan Pan, Yun Xu, and Jinquan Huang are with the College of Energy and Power Engineering, Nanjing University of Aeronautics and Astronautics, Nanjing 210016, China (e-mail: muxuan.pan@nuaa.edu.cn; xu_yun_nuaa@nuaa.edu.cn; jhuang@nuaa.edu.cn).

Binbin Gu is with the Aero Engine Control Systems Institute, Wuxi 214062, China (e-mail: binbin_gu@nuaa.edu.cn).

Ye-Hwa Chen is with the George W. Woodruff School of Mechanical Engineering, Georgia Institute of Technology, Atlanta, GA 30332-0405 USA (e-mail: yehwa.chen@me.gatech.edu).

Color versions of one or more figures in this article are available at <https://doi.org/10.1109/TIE.2021.3095784>.

Digital Object Identifier 10.1109/TIE.2021.3095784

improvements in engine performance, such as higher thrust-weight ratio, economic efficiency, and security, aircraft engines have become increasingly sophisticated. This sophistication has enhanced the inherent and significant coupling and promoted the development of multivariable control.

Wider operating and environmental conditions have strengthened the nonlinearity of engine dynamics. For the control design of such complex systems, one early approach was to linearize this nonlinear system under a fixed operating condition. A state variable model (SVM) could be formulated from the component-level thermodynamic model [2]. However, modeling errors, individual differences, inlet distortion, and component deterioration presented new challenges to the full authority digital engine control (FADEC) of aircraft engines [2], [3].

To address these challenges, efforts have been devoted to robust control design. A linear-quadratic regulator (LQR) was adopted for the F100 aircraft engine to account for multiple loop interactions and optimize engine performance [4]. The LQR control design relies on nominally linear models. However, when the uncertainty causes a significant deviation of the dynamics between the actual system and its (nominally) linear model, the efficacy of the LQR controller may deteriorate. To compensate for this uncertainty, one can introduce an assumption of matching conditions to the uncertainty (that is, the uncertainty lies within the range space of the input matrix), and linear and nonlinear control design may follow [5], [6]. Along this line, an uncertainty and disturbance estimator (UDE) for multivariable engine control systems was proposed [7]. In these applications, the uncertainty is prescribed by its bound and is assumed to be matched. That is, the (crisp) information of the uncertainty bound should be known. However, the uncertainty, including modeling errors, is likely to exhibit various bound characteristics that depend on the operating conditions. This suggests that describing the uncertainty bound by classes with different degrees (hence fuzzy) should be more practical and feasible.

The fuzzy dynamic system approach proposes a rather different angle on the union of the fuzzy theory and the Leitmann approach [25] from the IF–THEN rule-based control [26], [27]. Fuzzy-described uncertainty is explored, and non-IF–THEN rule-based robust control is proposed to achieve deterministic performance. This is quite different from the crisp-bound assumption or uncertainty estimation approach [28], [29]. This new approach also has been extended to mechanical

systems [30]. It can be noted that in these previous studies, the uncertainty considered in fuzzy dynamic systems is required to satisfy the matching conditions. However, in turbofan engine control systems, the uncertainty cannot meet the matching conditions due to the different dimensions between states and inputs. The historical controller design methods for the system with mismatched uncertainty are focus on the sliding-mode control [31], [32], the back-stepping control [33], and the rising neural network control [34].

In this article, a creative approach that can address the mismatched uncertainty for the aircraft engines is proposed. The system is divided into nominal systems and uncertainty portions. For the nominal system, a classic robust control is designed to render the baseline performances, including uniform boundedness and uniform ultimate boundedness. The uncertainty consists of two portions, namely, the matched uncertainty and the mismatched uncertainty, the bounds of which lie within prescribed fuzzy sets. There is a design parameter in the control, whose value needs to be feasible, and hence it falls within a range. To explore the optimal choice of this parameter, the performance threshold is addressed, which is due to both matched and mismatched uncertainty. By casting the performance into a fuzzy-theoretic setting and in combination with control cost, an integrated cost index is proposed. Then an optimization problem is formulated, which chooses the control design parameter among the feasible options to minimize the cost index. The solution to this optimization problem is shown to be both *existent* and *unique*. Therefore, this problem can be completely solved. The resulting control guarantees baseline performances regardless of the actual value of the uncertainty. In addition, the cost index is minimized.

The salient novelties and contributions of this approach are fourfold. First, the fuzzy-bounding information of the *matched* uncertainty is utilized in forming the *feasible* robust control. Second, the fuzzy-bounding information of the *mismatched* uncertainty is meticulously blended with the system performance and control efforts to form an integrated cost index, which reflects the comprehensive considerations for control design. This approach to the mismatched uncertainty was never addressed before and is novel. Third, the proposed optimization problem is both practical and tractable. As a result, all performance requirements, including uniform boundedness, uniform ultimate boundedness, and optimality are made possible by one *unique* design. Fourth, the hardware-in-the-loop (HIL) laboratory testing is conducted and the results demonstrate the superiority and practicality of the control.

The rest of the article is organized as follows. In Section II, a fuzzy dynamic system with uncertainty is formulated, which consists of matched and mismatched parts. In Section III, a multivariable robust controller is proposed and proven to render the resulting closed system uniformly bounded and uniformly ultimately bounded. In Section IV, an optimal control gain is pursued subject to a comprehensive performance index with transient responses, steady performance and controlled cost. In Section V, a control application for turbofan engines is presented. The HIL laboratory tests demonstrate the effective real-time

performances of the new control in the entire flight envelope. Section VI concludes this article.

II. UNCERTAIN FUZZY DYNAMIC SYSTEMS

An uncertain system can be described as

$$\dot{x}(t) = (A + \Delta A(x(t), \sigma(t), t))x(t) + (B + \Delta B(x(t), \sigma(t), t))u(t) \quad (1)$$

$$x(t_0) = x_0. \quad (2)$$

Here, $t \in \mathbb{R}$ is the time, $x(t) \in \mathbb{R}^n$ is the state, x_0 is the initial state, $\sigma(t) \in \mathbb{R}^p$ is an unknown parameter, $u(t) \in \mathbb{R}^m$ is the input, $A \in \mathbb{R}^{n \times n}$ is the nominal system matrix, and $B \in \mathbb{R}^{n \times m}$ is the nominal input matrix. The functions $\Delta A(\cdot)$ and $\Delta B(\cdot)$ are continuous. If $\Delta A(\cdot) \equiv 0$ and $\Delta B(\cdot) \equiv 0$, system (1) is called *the nominal system*.

Note that the uncertain system is represented via an explicit and deterministic mathematical form. It is not based on IF-THEN fuzzy rules (as in, e.g., the Takagi–Sugeno fuzzy model).

Assumption 1: The system (A, B) is stabilizable.

Consider the algebraic Riccati equation (ARE) [35]

$$A^T P + PA - 2PBR^{-1}B^T P + Q = 0 \quad (3)$$

where $Q > 0$ and $R > 0$ are matrices with appropriate dimensions. If (A, B) is stabilizable, the solution $P > 0$ to (3) exists and is unique. This assumption imposes a suggestion on how one chooses the nominal system. The rest of the system can be lumped into ΔA and ΔB .

Assumption 2: Consider the entry x_{0i} of x_0 and the entry σ_i of σ , $i = 1, 2, \dots, n$. There are fuzzy sets \mathcal{X}_{0i} and \mathcal{S}_i in universes of discourse $\mathbb{X}_i \in \mathbb{R}$ and $\mathbb{S}_i \in \mathbb{R}$, respectively. The membership functions of x_{0i} and σ_i are $\nu_{\mathbb{X}_i} : \mathbb{X}_i \rightarrow [0, 1]$ and $\mu_i : \mathbb{S}_i \rightarrow [0, 1]$. That is,

$$\mathcal{X}_{0i} = \{(x_{0i}, \nu_{\mathbb{X}_i}(x_{0i})) | x_{0i} \in \mathbb{X}_i\} \quad (4)$$

$$\mathcal{S}_i = \{(\sigma_i, \mu_i(\sigma_i)) | \sigma_i \in \mathbb{S}_i\} \quad (5)$$

where \mathbb{X}_i and \mathbb{S}_i are compact and known.

Remark 1: This assumption means that the (unknown) initial condition and uncertain parameter lie within a prescribed fuzzy set [25]. The engineering uncertainty can be analyzed via observed and measured data and can be described by expert statements. Generally, the data are limited. In addition, due to the ambient environments and personal customs, the operation cannot be repeated under the same conditions. For example, aircraft engines are disturbed by environmental conditions, which are difficult to replicate. Therefore, the frequency of occurrence information of certain conditions based on a large number of repetitions is sometimes limited. This in turn suggests that any realistic probability information may be hard to obtain. Alternatively, expert statements and common sense might work, and fuzzy set theory can be applied to the description of uncertainty, such as “the disturbance is small.” More discussions of this subject can be found in [36].

Now, decompose the uncertainty. Choose matrices $D(x, \sigma, t)$, $\Delta\tilde{A}(x, \sigma, t)$, $E(x, \sigma, t)$, and $\Delta\tilde{B}(x, \sigma, t)$ that satisfy

$$\Delta A(x, \sigma, t) = BD(x, \sigma, t) + \Delta\tilde{A}(x, \sigma, t) \quad (6)$$

$$\Delta B(x, \sigma, t) = BE(x, \sigma, t) + \Delta\tilde{B}(x, \sigma, t) \quad (7)$$

where the matrices D and E can be interpreted as the matched part of uncertainty, and $\Delta\tilde{A}$ and $\Delta\tilde{B}$ can be interpreted as the mismatched part of uncertainty [37].

Assumption 3: i) There exist fuzzy numbers ρ_D , ρ_{E2} , and ρ_{E1} such that for all $(x, \sigma, t) \in \mathbb{R}^n \times \mathbb{S} \times \mathbb{R}$ with $\mathbb{S} = \mathbb{S}_1 \times \mathbb{S}_2 \times \dots \times \mathbb{S}_p$

$$\|D(x, \sigma, t)\| \leq \rho_D \quad (8)$$

$$\frac{1}{2}\lambda_m(E(x, \sigma, t)R^{-1} + R^{-1}E^T(x, \sigma, t)) \geq \rho_{E1} > -\lambda_m(R^{-1}) \quad (9)$$

$$\|E(x, \sigma, t)\| \leq \rho_{E2} \quad (10)$$

where λ_m (λ_M) is the minimum (maximum) eigenvalue of the designated matrix.

ii) For ρ_D , ρ_{E1} and ρ_{E2} , fuzzy sets P_D , P_{E1} , and P_{E2} exist in the universes of discourse $\Psi_D \in \mathbb{R}$, $\Psi_{E1} \in \mathbb{R}$, and $\Psi_{E2} \in \mathbb{R}$ by the membership functions $\mu_D : \Psi_D \rightarrow [0, 1]$, $\mu_{E1} : \Psi_{E1} \rightarrow [0, 1]$, $\mu_{E2} : \Psi_{E2} \rightarrow [0, 1]$.

Since the designated matrix is always symmetric in this article, all eigenvalues of the matrix are real, hence, λ_m (λ_M) always exists.

Remark 2: Assumption 3 means that the uncertainty bound is prescribed by fuzzy information (for example, one may say the bound is “small,” where “small” is a linguistic variable associated with a membership function). This renders the past “hard bound” prescription (for example, the bound is 1), a special case of the fuzzy prescription since now the “hard bound” is viewed as a crisp number.

Remark 3: The fuzzy numbers ρ_D , ρ_{E1} , and ρ_{E2} can be evaluated since their universes of discourse are known. $\rho_{E1} > -\lambda_m(R^{-1})$ means that the direction of the control is not reversed even in the presence of uncertainty.

Now the mismatched uncertainty is addressed, which has never been discussed before in the context of fuzzy dynamic systems.

Assumption 4: For all $(x, \sigma, t) \in \mathbb{R}^n \times \mathbb{S} \times \mathbb{R}$

$$\lambda_m(Q) - \lambda_M(\Delta\tilde{A}^T(x, \sigma, t)P + P\Delta\tilde{A}(x, \sigma, t)) > 0 \quad (11)$$

$$\frac{1}{2}\lambda_m(BR^{-1}\Delta\tilde{B}^T(x, \sigma, t) + \Delta\tilde{B}(x, \sigma, t)R^{-1}B^T) \geq 0. \quad (12)$$

Remark 4: This assumption means that the magnitude of the mismatched uncertainty $\Delta\tilde{A}$ is within a threshold. In the special case when the uncertainty ΔA is matched, then $\Delta\tilde{A} \equiv 0$ and $\lambda_M = 0$. Therefore, (11) is always met since $\lambda_m(Q) > 0$. The mismatched uncertainty $\Delta\tilde{B}$ is to be “coherent with” the nominal input matrix B in the sense that they point in the same direction (i.e., $\lambda_m \geq 0$). In the special case when the uncertainty ΔB is matched, then $\Delta\tilde{B} \equiv 0$ and $\lambda_m = 0$. Therefore, (12) is always met.

Remark 5: Some comprehensive physical systems are too complex to be modeled by explicit mathematical functions. For instance, for aircraft engines, the performance characteristics of compressors and turbines are normally obtained by tests. These test results are generally discrete and nonlinear. Knowing the explicit relationship between the uncertain parameter σ and the matrices A , B , ΔA , ΔB is difficult. Assumption 3 provides an effective way to solve these problems. Therefore, the bound of uncertainty is used for analysis instead.

III. FEASIBLE ROBUST CONTROL DESIGN

A class of feasible robust controllers is proposed as follows:

$$u(t) = -R^{-1}B^T Px(t) - \gamma \|x(t)\|^2 R^{-1}B^T Px(t) \quad (13)$$

where $\gamma > 0$ is a constant.

This controller is deterministic in the sense that it is represented via an explicit mathematical expression. It is not based on IF-THEN fuzzy rules (as in, e.g., a Mamdani type architecture). There are two portions in $u(t)$. The first one, namely, $-R^{-1}B^T Px(t)$, is designed for the nominal system. Once the solution $P > 0$ to (3) is calculated, the control input direction $-R^{-1}B^T P$ is prescribed. The second portion compensates for the effect of uncertainty. The direction of this component, $-R^{-1}B^T P$, is the same as that of the first portion. Its gain is related to the norm of states and the design parameter γ , whose only requirement is strict positiveness.

Theorem 1: Consider system (1) subjected to Assumptions 1–4. Suppose controller (13) is applied to system (1). The solution of the controlled system is uniformly bounded and uniformly ultimately bounded.

Proof: Consider the Lyapunov function candidate

$$V = x^T Px \quad (14)$$

where P is the solution of the ARE (3). The time derivative of V along the trajectory of the controlled system (1) is

$$\begin{aligned} \dot{V} &= \dot{x}^T Px + x^T P \dot{x} \\ &=: \dot{V}_1 + \dot{V}_2 \end{aligned} \quad (15)$$

where

$$\begin{aligned} \dot{V}_1 &= 2x^T A^T Px + 2u^T B^T Px \\ &\quad + 2x^T D^T B^T Px + 2u^T E^T B^T Px \end{aligned} \quad (16)$$

$$\dot{V}_2 = 2x^T \Delta\tilde{A}^T Px + 2u^T \Delta\tilde{B}^T Px. \quad (17)$$

Note that the mismatched parts are “lump” in \dot{V}_2 .

For simplicity of notations, let $h := \gamma \|x(t)\|^2$, and $\hat{\alpha} := B^T Px$. Introducing (1) and (13) into (16) and posing Assumption 3 and Assumption 4 on the result, there is

$$\begin{aligned} \dot{V}_1 &= x^T (A^T P + PA - 2PBR^{-1}B^T P) x \\ &\quad - 2h\hat{\alpha}^T R^{-1}\hat{\alpha} + 2x^T D^T B^T Px - 2x^T PBR^{-1}E^T \hat{\alpha} \\ &\quad - h\hat{\alpha}^T (ER^{-1} + R^{-1}E^T) \hat{\alpha} \\ &\leq -\lambda_m(Q) \|x\|^2 + \frac{(\rho_D + \rho_{E2} \|R^{-1}B^T P\|)^2 \|x\|^2}{2(\rho_{E1} + \lambda_m(R^{-1}))h} \\ &= -\lambda_m(Q) \|x\|^2 + \frac{\theta}{\gamma} \end{aligned} \quad (18)$$

where $\theta := \frac{\bar{a}^2}{2(\rho_{E1} + \lambda_m(R^{-1}))}$ and $a := \rho_D + \rho_{E2}\|R^{-1}B^T P\|$.

Remark 6: The fuzzy numbers \bar{a} and θ are related to ρ_D , ρ_{E1} , and ρ_{E2} . Their membership functions can be calculated via μ_D , μ_{E1} , μ_{E2} and the fuzzy mathematics [38].

Now, consider the uncertain part \dot{V}_2 . Introduce (13) into (17) and let $\hat{\beta} := Px$. By Assumption 4, it yields

$$\begin{aligned} \dot{V}_2 &= 2x^T \Delta \tilde{A} P x \\ &\quad + 2 \left(-\hat{\beta}^T B R^{-1} \Delta \tilde{B}^T \hat{\beta} - h \hat{\beta}^T B R^{-1} \Delta \tilde{B}^T \hat{\beta} \right) \\ &\leq 2x^T \Delta \tilde{A} P x. \end{aligned} \quad (19)$$

Let $\Lambda := \lambda_m(Q) - \lambda_M(\Delta \tilde{A}^T P + P \Delta \tilde{A})$ and T is the membership function of Λ . Combine (18) and (19). Finally,

$$\dot{V} = \dot{V}_1 + \dot{V}_2 \leq -\Lambda \|x\|^2 + \frac{\theta}{\gamma}. \quad (20)$$

By (20) and the main consequence of [39], the solution of the controlled system (1) is uniformly bounded and uniformly ultimately bounded.

Remark 7: One of the main differences between this article and [25], [40] is that, in this article, the mismatched uncertainty is considered and described by fuzzy sets due to the fuzzy uncertain parameter σ . Therefore, the parameter Λ in (20) is also a fuzzy number. To satisfy (11), Λ should be positive. For the given pair (P, Q) , the positive membership function T of Λ guarantees the positive definiteness of Λ . In a specific application, T should be checked.

The inequality (20) implies that \dot{V} is negative for all $\|x\| > \Omega$ with $\Omega = \sqrt{\frac{\theta}{\gamma\Lambda}}$. For system (1), if $\|x_0\| \leq r$, the boundedness $d(r)$ of the solution $x(t)$ can be given as

$$d(r) = \begin{cases} \sqrt{\frac{\lambda_M(P)}{\lambda_m(P)}} \Omega, & \text{if } r < \Omega \\ \sqrt{\frac{\lambda_M(P)}{\lambda_m(P)}} r, & \text{if } r \geq \Omega \end{cases}. \quad (21)$$

In control (13), any design parameter $\gamma > 0$ is feasible in the sense of rendering uniform boundedness and uniform ultimate boundedness. A larger γ results in a larger magnitude of $u(t)$. If Q and R in (21) are selected and uncertainties are characterized by given membership functions, then P , θ , and Λ are determined. Under this situation, the parameter γ can be used to regulate the size of $d(r)$. For example, a larger γ causes a smaller boundedness. This contradictory influence of γ suggests a trade-off between the control cost and performance. Hence, an optimal design for γ is attractive and will be pursued in the next section.

IV. OPTIMAL GAIN

By increasing γ , the uniform ultimate boundedness region decreases, which implies stronger performance. However, the trade-off is that the control effort increases. For a physical system, the hardware constraints prevent all conflicting criteria from reaching the limitations. These limitations encourage designers to seek an optimal γ and achieve the desired performance of controlled systems. Here, some preparations are first presented before introducing the optimal index.

Let

$$\begin{aligned} j_s(\theta, \gamma, \tau, t_s) &= \left(V_s - \frac{\lambda_M(P)}{\Lambda} \frac{\theta}{\gamma} \right) \exp \left[-\frac{\Lambda}{\lambda_M(P)} (\tau - t_s) \right] \end{aligned} \quad (22)$$

$$j_\infty(\theta, \gamma) = \frac{\lambda_M(P)}{\Lambda} \frac{\theta}{\gamma}, \quad (23)$$

where $V_s = x(t_s)^T P x(t_s)$, and the time t_s is the instant that the controller starts to work. Equations (22) and (23) represent the system transient and steady-state performances, respectively. Since the value of uncertainty is difficult to identify exactly, a practical method is to utilize $j_s(\theta, \gamma, \tau, t_s)$ and $j_\infty(\theta, \gamma)$ to analyze these performances. The indexes $j_s(\theta, \cdot)$ and $j_\infty(\theta, \cdot)$ depend on the fuzzy number θ , which can be evaluated by its membership function.

Definition 1: Consider a fuzzy set

$$\mathcal{V} = \{(\xi, \mu_{\mathbb{V}}(\xi)) \mid \xi \in \mathbb{V}\}. \quad (24)$$

For any function $g(\cdot) : \mathbb{V} \rightarrow \mathbb{R}$, the \mathcal{D} -operation $\mathcal{D}[g(\xi)]$ is given by

$$\mathcal{D}[g(\xi)] = \frac{\int_{\mathbb{V}} g(\xi) \mu_{\mathbb{V}}(\xi) d\xi}{\int_{\mathbb{V}} \mu_{\mathbb{V}}(\xi) d\xi}. \quad (25)$$

Remark 8: The \mathcal{D} -operation is the average value of $g(\xi)$ over $\mu_{\mathbb{V}}(\xi)$ for defuzzification. Compared to the center of gravity defuzzifier, which can be considered the reduced case where $g(\xi) = \xi$, the \mathcal{D} -operation is more general and can defuzzify the results of fuzzy arithmetic [41].

Now, the following performance cost function

$$\begin{aligned} J(\gamma, t_s) &= \mathcal{D} \left[\int_{t_s}^{\infty} j_s^2(\theta, \gamma, \tau, t_s) d\tau \right] + \alpha \mathcal{D} [j_\infty^2(\theta, \gamma)] + \beta \gamma^2 \\ &=: J_1(\gamma, t_s) + \alpha J_2(\gamma) + \beta J_3(\gamma) \end{aligned} \quad (26)$$

is proposed, where the weighting factors α and $\beta > 0$ are constants.

Remark 9: The reason for choosing J is threefold. First, J_1 addresses the transient performance threshold (in the sense of the fuzzy \mathcal{D} -operation). Second, J_2 addresses the average (in the sense of the fuzzy \mathcal{D} -operation) of the steady-state performance. Third, J_3 addresses the control *cost* through the magnitude γ . With the combination of J_1 , J_2 , and J_3 , the cost function J could provide the most comprehensive assessment of the system performance and the required cost.

Let $\kappa := \frac{\lambda_M(P)}{\Lambda}$, and (26) can be rewritten as

$$J(\gamma, t_s) = \kappa_1 - \frac{\kappa_2}{\gamma} + \frac{\kappa_3}{\gamma^2} + \alpha \frac{\kappa_4}{\gamma^2} + \beta \gamma^2 \quad (27)$$

where $\kappa_1 = \frac{1}{2} \mathcal{D}[\kappa V_s^2]$, $\kappa_2 = \mathcal{D}[\kappa^2 V_s \theta]$, $\kappa_3 = \frac{1}{2} \mathcal{D}[\kappa^3 \theta^2]$, $\kappa_4 = \mathcal{D}[\kappa^2 \theta^2]$. By the \mathcal{D} -operation, $\kappa_i, i = 1, 2, 3, 4$, are definitely determined, and then the index $J(\cdot)$ is a polynomial depending on γ . Therefore, our gain optimization becomes a search for the optimal γ^* ($\gamma^* > 0$) by minimizing $J(\gamma, t_s)$. The constrained optimization problem of $J(\gamma, t_s)$ can be described as

$$\min_{\gamma} J(\gamma, t_s) \quad \text{s.t. } \gamma > 0 \quad (28)$$

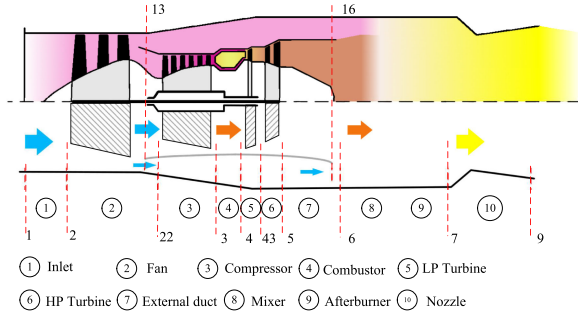


Fig. 1. Turbofan engine structural diagram.

for any $t_s \geq 0$. Letting $\partial J / \partial \gamma = 0$ (this is a *necessary* condition to the optimization problem) yields

$$\kappa_2 \gamma + 2\beta \gamma^4 = 2\kappa_3 + 2\alpha \kappa_4. \quad (29)$$

The solution to (29) serves as a candidate solution to the optimization problem. For given $\kappa_{3,4} > 0$, the left-hand side is monotonically increasing with γ . As a result, the solution $\gamma^* > 0$ to (29) exists and is globally unique. As $\gamma = \gamma^*$, $\partial^2 J / \partial \gamma^2 = (1/\gamma^{*3})(\kappa_2 + 8\beta \gamma^{*3}) > 0$ (this is a *sufficient* condition for the optimization problem). Therefore γ^* is indeed the solution.

As a result of both the analyses of the *necessary* condition and *sufficient* condition, the *global unique* solution to the optimization problem (28) is guaranteed to exist. The optimization problem is therefore solved.

The procedure of the control design is summarized as follows.

- 1) For given $Q > 0$, $R > 0$, solve the Riccati equation (3).
- 2) Choose fuzzy sets ρ_{E1} , ρ_{E2} , ρ_D , and ρ_w . Calculate κ_i ($i = 1, 2, 3, 4$) based on the α -cut of the membership function, fuzzy arithmetic, and the decomposition theorem.
- 3) For given $\alpha, \beta > 0$, calculate $\gamma^* > 0$ in (29).
- 4) The robust control scheme is obtained by (13).

Remark 10: Since $R > 0$ and the parameter γ^* is existent and globally unique, there is no singularity in the calculation of the robust control (13).

V. APPLICATION TO TURBOFAN ENGINE

A. Fuzzy Dynamic System of Turbofan Engine

Consider a turbofan engine shown in Fig. 1. The fuzzy dynamic system of the engine can be described as (1) and

$$x(t) = \left[n_L(t) \ n_H(t) \ \int_{t_0}^t e_1(\tau) d\tau \ \int_{t_0}^t e_2(\tau) d\tau \right]^T \quad (30)$$

$$u(t) = [W_f(t) \ A_8(t)]^T \quad (31)$$

$$e_1(t) = n_{Hr}(t) - n_H(t), \ e_2(t) = EPR_r(t) - EPR(t) \quad (32)$$

where $n_L(t)$ and $n_H(t)$ are the speeds of the low-pressure (LP) rotor and high-pressure (HP) rotor, $EPR(t)$ is the engine pressure ratio, $n_{Hr}(t)$ and $EPR_r(t)$ are references to $n_H(t)$ and $EPR(t)$, respectively, and $W_f(t)$ and $A_8(t)$ are the main fuel flow and the nozzle throat area, respectively.

Because the input matrix B is not a square matrix,

$$D := (B^T B)^{-1} B^T \Delta A \quad (33)$$

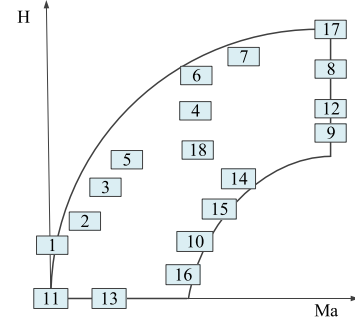


Fig. 2. Envelope of a turbofan engine.

$$E := (B^T B)^{-1} B^T \Delta B \quad (34)$$

are defined and the uncertainty of the turbofan can be depicted as (6) and (7).

Remark 11: The characteristic parameters of engines are solved by a series of iterations that form an engine component-level model based on mechanical, fluid mechanics, and thermodynamic principles [2]. For the control design in this article, SVMs are needed and extracted from the component-level model by perturbation and/or fitting approaches. Hence, uncertain matrices ΔA and ΔB are utilized to describe the uncertainty and nonlinearity and adopt fuzzy sets to describe their bounds.

Based on a turbofan nonlinear model, its SVMs are built as

$$\dot{x} = A_k x + B_k u, \ x_0 = x(t_0), \ k = 1, 2, \dots, N_p \quad (35)$$

at N_p operation points in the flight envelope as shown in Fig. 2. Here, H is the flight height and Ma is the flight Mach number. The matrices A_k and B_k are collected and their averages are taken as A and B . That is,

$$A = \frac{1}{N_p} \sum_{k=1}^{N_p} A_k, \ B = \frac{1}{N_p} \sum_{k=1}^{N_p} B_k. \quad (36)$$

Let

$$\Delta A = \omega_1 A, \ \Delta B = \omega_2 B. \quad (37)$$

Here, ω_1 and ω_2 are fuzzy sets, which indicate “how small the system uncertainty is.” For the entries in ΔA and ΔB , there are

$$\Delta \bar{a}_{ij} := \frac{a_{ij} - a_{ij,k}}{a_{ij}}, \ \Delta \bar{b}_{ij} := \frac{b_{ij} - b_{ij,k}}{b_{ij}} \quad (38)$$

$$\sigma_1 := \max_{i,j} \Delta \bar{a}_{ij}, \ \sigma_2 := \max_{i,j} \Delta \bar{b}_{ij} \quad (39)$$

and the associated membership functions are ($i = 1, 2$)

$$\mu_{\omega_i}(\sigma_i) = \begin{cases} 1 - \frac{\sigma_i}{\bar{m}_i} & 0 \leq \sigma_i \leq \bar{m}_i \\ 1 - \frac{\sigma_i}{\underline{m}_i} & \underline{m}_i \leq \sigma_i \leq 0 \end{cases} \quad (40)$$

where \bar{m}_i , \underline{m}_i , are given constants. By (6), (7), (33), (34), and (37),

$$\rho_D \geq \omega_1 \left\| B^T (B^T B)^{-1} A \right\| \quad (41)$$

$$\rho_{E1} \leq \omega_2 \lambda_m (R^{-1}) \quad (42)$$

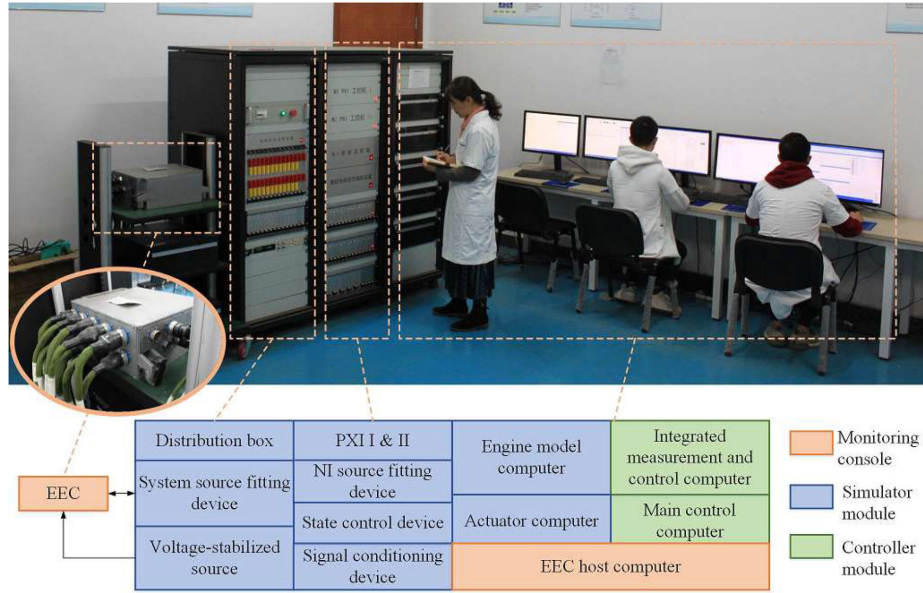


Fig. 3. Aircraft engine HIL simulator.

$$\rho_{E2} \geq |\omega_2|. \quad (43)$$

Assumption 3 is met. Thus far, the fuzzy dynamic system for a turbofan has been formed. By the robust control (13), the controlled engine system is uniformly bounded and ultimately uniformly bounded by Theorem 1.

B. HIL Engine Simulator and Laboratory Testing

HIL simulation is a real-time technique that is used in the development and test of complex system. HIL simulation provides an effective platform by adding the complexity of the system under control to the test platform [42]. To demonstrate the performances of the proposed robust control (13), HIL laboratory testing is performed on the aircraft engine HIL simulator shown in Fig. 3. The HIL simulator in our laboratory consists of three main parts.

1) *The Controller Module*: The electronic engine control (EEC) unit, the core of the HIL simulator, is physical hardware applied to a turbofan engine. The designed control algorithm, operating in the EEC, is design by C code and downloaded from the EEC host computer to the EEC by automatic code generation of the software *Matlab/Simulink*. These two parts comprise the controller module.

2) *The Simulator Module*: The module contains the actuator computer, the engine model computer, the peripheral component interconnect extension for instrumentation (PXI) industrial computers, the signal conditioning device, the state control device, the load simulator, the national instruments (NI) source-fitting device, and the system-fitting source-fitting device in the simulator module. It can not only simulate the steady and dynamic characteristics of the engine within the entire flight envelope but also simulate, collect, and display the real sensor signals and the actuator signals.

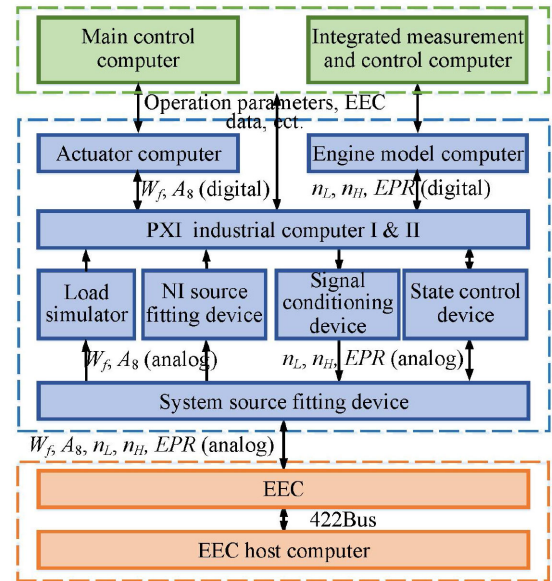


Fig. 4. Information transmission in the HIL simulator.

3) *The Monitoring Console*: The main control computer, the integrated measurement, and the control computer form the monitoring console. They display and record the current operation parameters of the engine, inputs, and outputs of the controller and alarm information. The main control computer schedules the testing tasks, such as the start/end of the EEC power and channel reset. An integrated measurement and control computer is used to collect and monitor the EEC data. The monitoring software is developed in VC++ 6.0.

The HIL tests implement in real time in a closed loop within the 25-ms control period as shown in Fig. 4. During the HIL

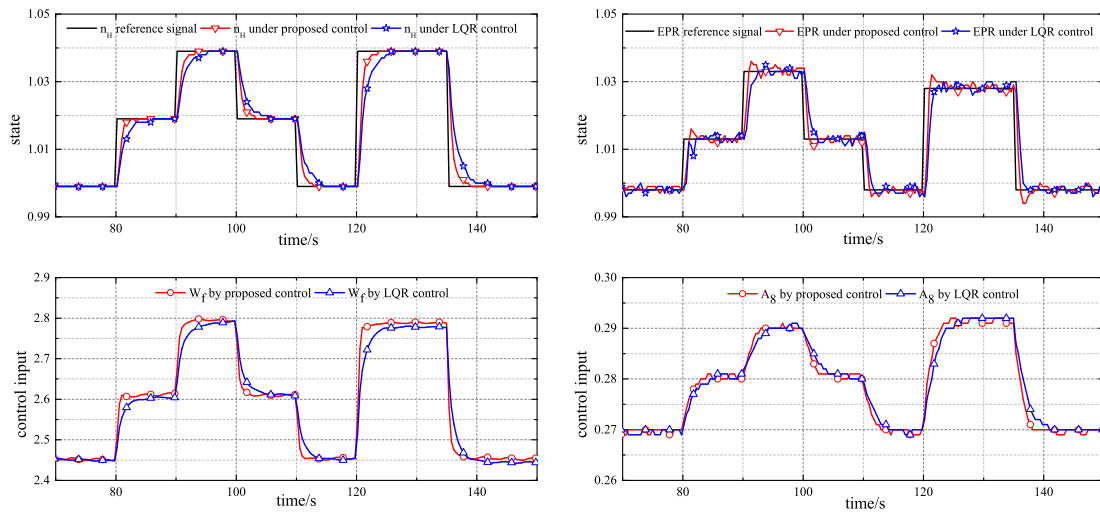


Fig. 5. HIL test results at (0, 0).

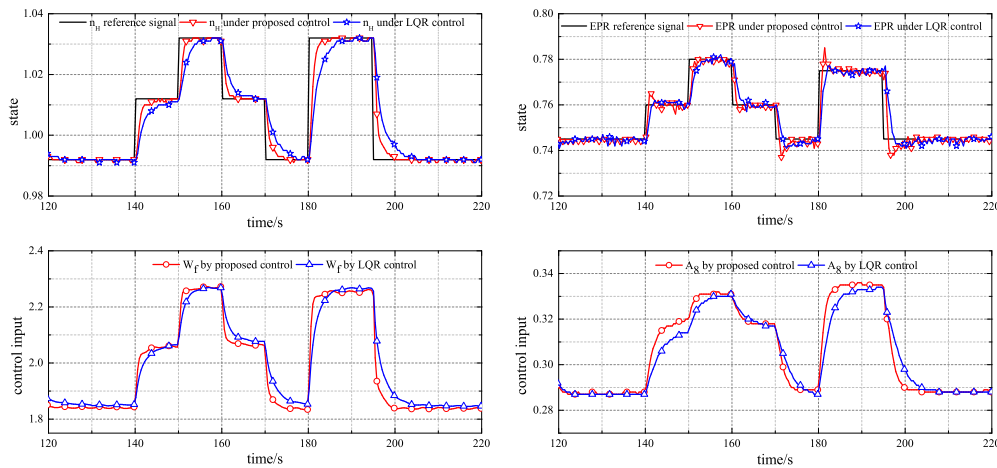


Fig. 6. HIL test results at (8, 1.4).

laboratory tests, the engine model computer and actuator computer calculate and send out the digital signals of W_f , A_8 , n_L , n_H , and EPR . By PXI industrial computers, load simulator, signal conditioning device, these digital signals are converted to the analog signals which have the same electrical characteristics with the physical sensors and actuators. The EEC samples the analog signals of n_L , n_H , and EPR and calculates and sends out the analog outputs W_f and A_8 .

The engine dynamics changes with the height, the Mach number, and its rotational speed; therefore, to testify the robustness of the proposed control, the computer simulations and HIL laboratory tests are conducted at the different points and a flight task cycle in the flight envelope. First, the tests are conducted at the points (0, 0) and (8, 1.4) in the flight envelope. In the tests, the references of steps n_H and EPR are shown as black lines in Fig. 5(a) and (b) and Fig. 6(a) and (b), and the test results are displayed in Figs. 5 and 6.

It can be concluded that with the new control, engine outputs n_H and EPR can track the references expeditiously and

effectively at different operation points, and the absolute steady errors are less than 0.5% in the presence of process noise and measurement noise in the HIL laboratory tests. Figs. 5(a) and 6(a) show that there are no overshoots of n_H responses under the proposed robust control at different operation points and that the settling times T_s of n_H are less than 2.0 s. The engine pressure ratio EPR responses have overshoots within 0.5%. It is noted that, at (0, 0), the uncertainty parameters ω_1 and ω_2 are 0.53 and 0.38, respectively. At (8, 1.4), they vary to 0.93 and 0.19. Figs. 5 and 6 also show that under the the proposed control, the n_H and EPR responses vary little and the controlled engine has excellent robustness regardless of the obvious variation of uncertainty.

An LQR control was imposed on the engine to compare the performances with the proposed robust control. There are three main reasons we chose LQR for comparison. First, LQR is the common control used in aircraft engines [4]–[7], besides the classical PID. Thus, it is desirable to see how our control prevails

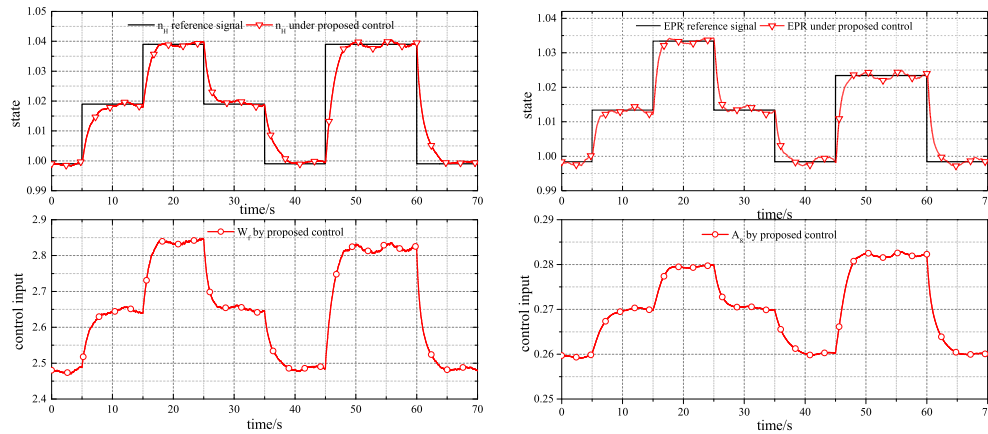


Fig. 7. Simulation results at (0, 0) with external disturbances.

over its counterparts in the same area. This is also the way other aircraft engine engineers are to perceive our contributions. Second, in practice, LQR is a standard test bed for comparisons, when it comes to new control developments (sliding mode, neural network, Sugeno–Takagi fuzzy systems, H_∞ , μ , l_1 , l_2 , adaptive, etc. [43], [44]). No other control has been tested and compared so extensively. This means our comparison can be easily extended to the comparisons with other advanced control designs. No other control can top LQR in this regard. Third, in theory, LQR is a well-studied robust control technique [45]. LQR has demonstrated robustness to parameter uncertainty and input channel uncertainty. We also address some new developments related to the LQR reliability in practice [46]–[48].

The LQR control conducted the same simulator procedure under the same operating conditions as that of the proposed control, and test results are also depicted in Figs. 5 and 6. In Figs. 5(a) and 6(a), it is found that there are also no overshoots under the LQR. Considering the settling time T_s of n_H responses, under the two control schemes, they are 1.78 and 2.98 s at (0, 0), and 1.58 and 3.80 s at (8, 1.4). Compared with the LQR, the settling time of the fuzzy control reduces by 40% at (0, 0) and by 58% at (8, 1.4). The acceptable overshoot threshold is 1%. The acceptable settling time threshold is 3.0 s. The overshoots under the two control scheme are both acceptable. The settling time T_s under the proposed control is about 40% under the threshold, whereas that of the LQR exceeds the threshold. The root-mean-square errors (RMSEs) of the n_H responses under the two control methods are 0.0042 and 0.0052 at (0, 0), and 0.0041 and 0.0053 at (8, 1.4). Compared with LQR, the RMSEs of the fuzzy control are reduced by 19% at (0, 0) and 23% at (8, 1.4). The EPR responses are both fast under these two controllers in Figs. 5(b) and 6(b). The histories of inputs W_f and A_8 are shown in Fig. 5(c) and (d) and Fig. 6(c) and (d). Moreover, to test the effect of external disturbance, an external disturbance $0.01 \times [1.8 \times (-0.5 + \text{rand}(1, 1)) + 0.1 \sin(t)]$ is injected into the n_H and EPR responses, respectively. Here, the $\text{rand}(1, 1)$ is a random in [0, 1] and the disturbance is in $[-0.01, 0.01]$, which is 10% of the magnitudes of n_H and EPR . This disturbance includes constant, sinusoidal, and random characteristics and is believed to reflect a very realistic scenario in

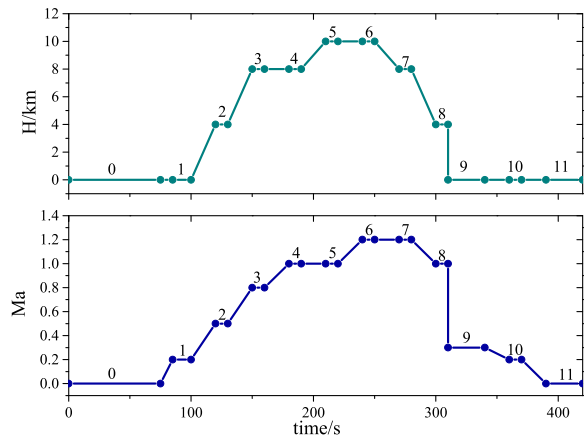


Fig. 8. Flight task cycle in the flight envelope.

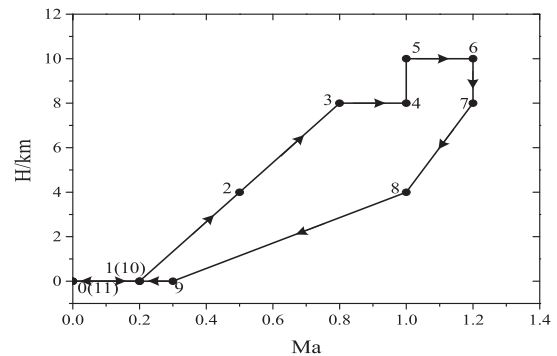


Fig. 9. Flight trajectory in the flight envelope.

practice. The control simulation is conducted at (0, 0) and the results are shown in Fig. 7. Fig. 7(a) and (b) shows that the n_H and EPR responses can track the references quickly and without steady-state errors. It can be concluded from these comparisons that, by the proposed optimum robust control, the controlled turbofan engine can achieve a good comprehensive performance in terms of transient and steady-state performance, control cost, and robustness.

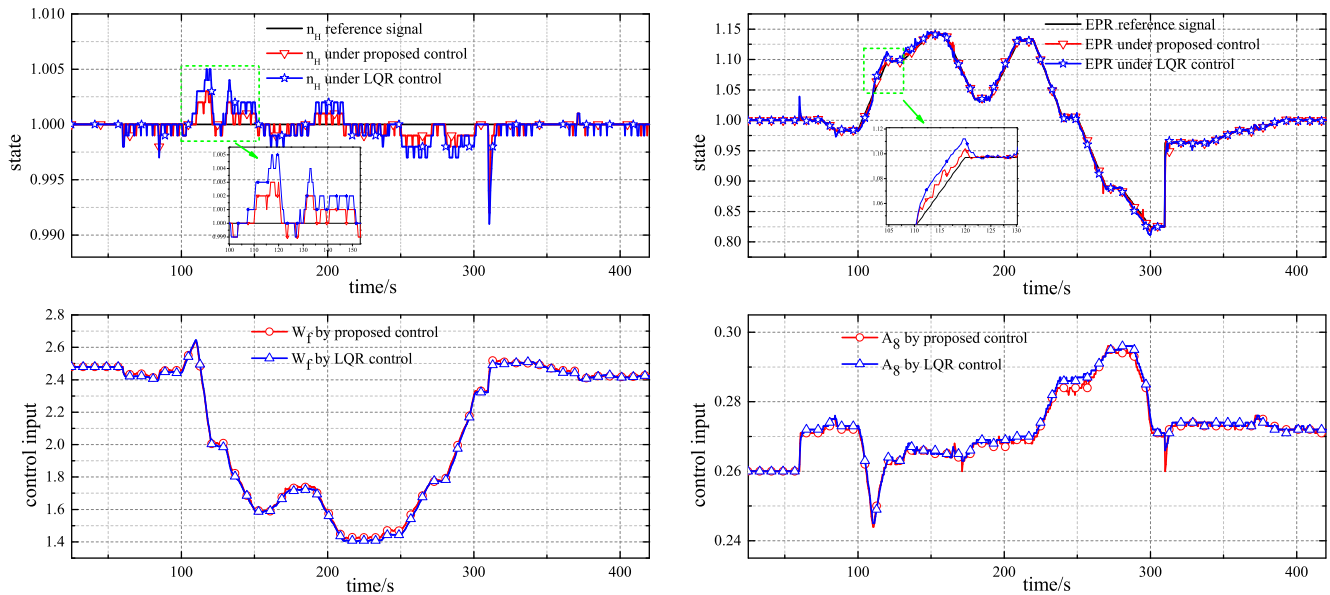


Fig. 10. HIL test results in the flight envelope.

Since turbofan engines continuously maneuver within the flight envelope and in order to testify the robustness of the controllers, the HIL laboratory tests simulating the actual flight process are further conducted. A flight task cycle is scheduled and described in Figs. 8 and 9. In the tests, the reference n_{Hr} is kept at 100%, and the flight height H and Mach number Ma vary continuously in the flight envelope. Fig. 10 shows the test results.

In Fig. 10(a), it can be seen that during the flight process, the output n_H varies with time by approximately 100% and the maximum deviation of n_H is approximately 0.8% because flight conditions H and Ma constantly change, which brings uncertainties. The curve in Fig. 10(a) has steps, which are generated by periodic sampling during the HIL laboratory tests. From the partially enlarged figure of Fig. 10(a), the maximum data disturbance of the proposed robust controller is 0.3%, while that of the LQR controller is 0.5%. The results indicate that the new robust controller has better robustness than the LQR scheme. Fig. 10(b) shows that the output of EPR under the new robust controller can track the reference EPR_r quickly when turbofan engines reach a stable state. The dynamic tracking error of the proposed controller is lower than that of the LQR method. Fig. 10(c) and (d) describes the control histories of W_f and A_8 .

VI. CONCLUSION

For controlling aircraft engines, there are two major challenges that have never been addressed. The first is that the uncertainty bound is *unknown*. The second is that there is *mismatched* uncertainty. A framework which constructively utilizes the characteristics of the two challenges was creatively proposed. The feasible robust control, which is based on any feasible design parameter $\gamma > 0$, was constructed to guarantee prescribed system performance regardless of the uncertainty.

The unsharp (fuzzy) uncertainty bound was used to formulate the performance threshold (J_1 and J_2), which incorporates the influence of both matched uncertainty and mismatched uncertainty. This performance threshold was then joined by the control effort, reflected by γ , to become the comprehensive performance index J . With this in hand, a constrained optimization problem was proposed.

The quest to solve this optimization problem was divided into two steps. The first step explored the use of the *necessary* condition for seeking all candidate solutions. It was found that there is only one candidate solution, which always exists. The second step explored the use of the *sufficient* condition to verify the candidate solution. It was shown that the only candidate solution passed the screening, and therefore is indeed the *global unique* solution to the optimization problem.

The resulting robust control scheme was applied to turbofan and HIL laboratory tests. The tests demonstrated that at two different operation points, the settling times T_s of n_H responses were 1.78 and 1.58 s under the proposed control which are reduced by 40% and 58% in comparison with the LQR. The tests of a flight cycle demonstrated that the proposed control exhibits effective robustness when considering the uncertainties caused by changes in flight conditions.

REFERENCES

- [1] L. C. Jaw and J. D. Mattingly, *Aircraft Engine Controls : Design, System Analysis, and Health Monitoring*. New York, NY, USA: American Institute of Aeronautics and Astronautics, 2009.
- [2] R. Hanz, *Advanced Control of Turbofan Engines*. New York, NY, USA: Springer Science and Business Media, 2011.
- [3] D. Esler, "FADEC's benefits today and tomorrow," *Bus. Commercial Aviation*, vol. 97, no. 5, pp. 90–108, Nov. 2005.
- [4] J. F. Soeder, "F100 Multivariable Control Synthesis Program: Computer Implementation of the F100 Multivariable Control Algorithm," Washington, DC, USA: NASA Center for Aerosp. Inf. (CASI), 1983.

- [5] M. Pan, L. Cao, W. Zhou, J. Huang, and Y. H. Chen, "Robust decentralized control design for aircraft engine: A fractional type," *Chin. J. Aeronaut.*, vol. 32, no. 2, pp. 347–360, Feb. 2019.
- [6] S. Yang, X. Wang, H. Wang, and Y. Li, "Sliding mode control with system constraints for aircraft engines," *ISA Trans.*, vol. 98, pp. 1–10, Mar. 2020.
- [7] L. Xiao, "Aeroengine multivariable nonlinear tracking control based on uncertainty and disturbance estimator," *J. Eng. Gas Turbines Power.*, vol. 136, no. 12, Dec. 2014, Art. no. 121601.
- [8] L. A. Zadeh, "Fuzzy sets," *Inf. Control.*, vol. 8, no. 3, pp. 338–353, 1965.
- [9] M. E. Hamdani, "Applications of fuzzy algorithms for control of simple dynamic plant," *Proc. Inst. Electr. Eng.*, vol. 121, no. 12, pp. 1585–1588, Dec. 1974.
- [10] R. Precup and H. Hellendoorn, "A survey on industrial applications of fuzzy control," *Comput. Ind.*, vol. 62, no. 3, pp. 213–226, Apr. 2011.
- [11] A. Nguyen, T. Taniguchi, L. Eciolaza, V. Campos, R. Palhares, and M. Sugeno, "Fuzzy control systems: Past, present and future," *IEEE Comput. Intell. Mag.*, vol. 14, no. 1, pp. 56–68, Feb. 2019.
- [12] S. Ifqir, I. Dalil, A. Naïma, and M. Said, "Adaptive threshold generation for vehicle fault detection using switched T-S interval observers," *IEEE Trans. Ind. Electron.*, vol. 67, no. 6, pp. 5030–5040, Jun. 2020.
- [13] X. Xie, H. Ma, Y. Zhao, D. W. Ding, and Y. Wang, "Control synthesis of discrete time T-S fuzzy systems based on a novel non-PDC control scheme," *IEEE Trans. Fuzzy Syst.*, vol. 21, no. 1, pp. 147–157, Feb. 2013.
- [14] M. Pan, H. Wang, B. Gu, X. Qiu, and Y. H. Chen, "A hierarchical robust control design with non-parallel distributed compensator and application to aircraft engines," *IEEE Access*, vol. 7, pp. 144813–825, Sep. 2019.
- [15] L. Wang, "A new look at Type-2 fuzzy sets and Type-2 fuzzy logic systems," *IEEE Trans. Fuzzy Syst.*, vol. 25, no. 3, pp. 693–706, Jun. 2017.
- [16] O. Castillo, L. Cervantes, J. Soriana, M. Sanchezb, and J. R. Castro, "A generalized type-2 fuzzy granular approach with applications to aerospace," *Inf. Sci.*, vol. 354, no. 1, pp. 165–177, Aug. 2016.
- [17] Y. Liu, R. Chen, X. Na, Y. Luo, and H. Zhang, "Robust fault estimation of vehicular yaw rate sensor using a Type-2 fuzzy approach," *IEEE Trans. Ind. Electron.*, vol. 68, no. 10, pp. 10029–10039, Oct. 2021.
- [18] X. Ping and W. Pedrycz, "Output feedback model predictive control of interval Type-2 T-S fuzzy system with bounded disturbance," *IEEE Trans. Fuzzy Syst.*, vol. 28, no. 1, pp. 148–162, Jan. 2020.
- [19] J. Zheng, "Adaptive fuzzy PID control for servo motor direct-drive pump control system," *J. Digit. Inf. Manag.*, vol. 12, no. 1, pp. 1–7, Feb. 2014.
- [20] J. Lai, H. Zhou, and W. Hu, "A new adaptive fuzzy PID control method and its application in FCBTM," *Int. J. Comput. Commun. Control.*, vol. 11, no. 3, pp. 394–404, Mar. 2016.
- [21] T. M. Guerra, A. Sala, and K. Tanaka, "Fuzzy control turns 50: 10 years later," *Fuzzy Sets Syst.*, vol. 281, pp. 168–182, Dec. 2015.
- [22] T. Takagi and M. Sugeno, "Fuzzy identification of systems and its applications to modeling and control," *IEEE Trans. Syst. Man Cybern.*, vol. 15 no. 1, pp. 116–132, Jan.–Feb. 1985.
- [23] P. Huek and K. Narenathreyas, "Aircraft longitudinal motion control based on Takagi–Sugeno fuzzy model," *Appl. Soft Comput.*, vol. 49, pp. 269–278, Dec. 2016.
- [24] K. Tanaka, H. Tsuyoshi, and H. Wang, "A multiple Lyapunov function approach to stabilization of fuzzy control systems," *IEEE Trans. Fuzzy Syst.*, vol. 11, no. 4, pp. 582–589, Aug. 2003.
- [25] Y. H. Chen, "A new approach to the control design of fuzzy dynamical systems," *J. Dyn. Syst. Meas. Control Trans. ASME*, vol. 133, no. 6, Nov. 2011, Art. no. 061019.
- [26] A. J. Chipperfield, B. Beatrice, and P. J. Fleming, "Fuzzy scheduling control of a gas turbine aero-engine: A multiobjective approach," *IEEE Trans. Ind. Electron.*, vol. 49, no. 3, pp. 536–548, Jun. 2002.
- [27] X. Chen, J. Hu, M. Wu, and W. Cao, "T-S fuzzy logic based modeling and robust control for burning-through point in sintering process," *IEEE Trans. Ind. Electron.*, vol. 64, no. 12, pp. 9378–9388, Dec. 2017.
- [28] L. B. Cosme, W. M. Caminhas, M. F. S. V. D'Angelo, and R. M. Palhares, "A novel fault-prognostic approach based on interacting multiple model filters and fuzzy systems," *IEEE Trans. Ind. Electron.*, vol. 66, no. 1, pp. 519–528, Jan. 2019.
- [29] H. Wu, "Robust stabilisation of uncertain time-delay dynamical systems with unknown bounds of uncertainties: A non-linear control method," *IET Control Theory Appl.*, vol. 9, no. 13, pp. 2039–2046, Aug. 2015.
- [30] H. Sun, R. Yu, Y. H. Chen, and H. Zhao, "Optimal design of robust control for fuzzy mechanical systems: Performance-based leakage and confidence-index measure," *IEEE Trans. Fuzzy Syst.*, vol. 27, no. 7, pp. 1441–1455, Jul. 2019.
- [31] J. Yang, S. H. Li, and X. H. Yu, "Sliding-mode control for systems with mismatched uncertainties via a disturbance observer," *IEEE Trans. Ind. Electron.*, vol. 60, no. 1, pp. 160–169, Jan. 2013.
- [32] J. Zhang, P. Shi, and Y. Xia, "Robust adaptive sliding-mode control for fuzzy systems with mismatched uncertainties," *IEEE Trans. Fuzzy Syst.*, vol. 18, no. 4, pp. 700–711, Aug. 2010.
- [33] W. Min and Q. Y. Liu, "An improved adaptive fuzzy backstepping control for nonlinear mechanical systems with mismatched uncertainties," *Automatika*, vol. 60, no. 1, pp. 1–10, Jan. 2019.
- [34] T. Ma, "Filtering adaptive neural network controller for multivariable nonlinear systems with mismatched uncertainties," *Int. J. Robust Nonlin.*, vol. 30, no. 12, pp. 4565–4583, Jul. 2020.
- [35] K. J. Astrom and R. M. Murray, *Feedback Syst.*, New York, NY, USA: Princeton University Press, 2008.
- [36] B. Kosko, "Fuzziness vs. probability," *Int. J. Gen. Syst.*, vol. 17, no. 2–3, pp. 211–240, Jun. 1990.
- [37] B. R. Barmish and G. Leitmann, "On ultimate boundedness control of uncertain systems in the absence of matching condition," *IEEE Trans. Autom. Control*, vol. 27, no. 1, pp. 153–158, Jan. 1982.
- [38] G. J. Klir and B. Yuan, *Fuzzy Sets and Fuzzy Logic: Theory and Applications*. Englewood Cliffs, NJ, USA: Prentice-Hall, 1995.
- [39] M. J. Corless and G. Leitmann, "Continuous state feedback guaranteeing uniform ultimate boundedness for uncertain dynamic systems," *IEEE Trans. Autom. Control*, vol. 26, no. 5, pp. 1139–1144, Oct. 1981.
- [40] Y. H. Chen and G. Leitmann, "Robustness of uncertain systems in the absence of matching assumptions," *Int. J. Control*, vol. 45, no. 5, pp. 1527–1542, May 1987.
- [41] D. P. Filev and R. R. Yager, "Three models of fuzzy logic controllers," *Cybern. Syst.*, vol. 24, no. 2, pp. 91–114, Jan. 1993.
- [42] R. T. Ogan, "Hardware-in-the-loop simulation," in *Model. and Simul. in the Syst. Eng. Life Cycle*. M. L. Loper, ed., London, U.K.: Loper Springer, 2015, p. 167.
- [43] K. Barya, S. Tiwari, and R. Jha, "Comparison of LQR and robust controllers for stabilizing inverted pendulum system," in *Proc. Int. Conf. Comm. Control Comput. Technol.*, Nagercoil, India, 2010, pp. 300–304.
- [44] M. Fakoor, S. Nikpay, and A. Kalhor, "On the ability of sliding mode and LQR controllers optimized with PSO in attitude control of a flexible 4-DOF satellite with time-varying payload," *Adv. Space Res.*, vol. 67, no. 1, pp. 334–349, Jul. 2021.
- [45] K. Zhou, J. C. Doyle, and K. Glover, *Robust and Optimal Control*. Englewood Cliffs, NJ, USA: Prentice Hall, 1995.
- [46] R. V. Vincent, J. Economou, D. G. Wall, and J. Cleminson, " H_∞ /LQR optimal control for a supersonic air-breathing missile of asymmetric configuration," *IFAC-PapersOnLine*, vol. 52, no. 12, pp. 214–218, Jan. 2019.
- [47] E. S. Barjuel and J. Ortiz, "A comprehensive performance comparison of linear quadratic regulator (LQR) controller, model predictive controller (MPC), H_∞ loop shaping and μ -synthesis on spatial compliant link-manipulators," *Int. J. Dyn. Control*, vol. 9, no. 1, pp. 121–140, Mar. 2021.
- [48] Y. Li, M. Xu, J. Chen, and X. Wang, "Nonprobabilistic reliable LQR design method for active vibration control of structures with uncertainties," *AIAA J.*, vol. 56, no. 6, Jun. 2018.



Muxuan Pan received the B.S. degree in flight vehicle power engineering, the M.S. degree in system simulation and control, and the Ph.D degree in aerospace propulsion theory and engineering from the Nanjing University of Aeronautics and Astronautics, Nanjing, China, in 2000, 2003, and 2011, respectively.

She is currently an Associate Professor with the Nanjing University of Aeronautics and Astronautics. Her research interests include robust control of uncertain systems, networked control systems, fuzzy control, and dynamic system modeling.



Yun Xu received the B.S. degree in flight vehicle power engineering in 2017 from the Nanjing University of Aeronautics and Astronautics, Nanjing, China, where he is currently working toward the Ph.D. degree in aerospace propulsion theory and engineering.

His research interests include fuzzy modeling, robust control, fuzzy control, and networked control for aircraft engines.



Jinquan Huang received the B.S. degree in control theory from Shandong University, Jinan, China, in 1984, and the M.S. degree in engine control engineering and the Ph.D. degree in aerospace propulsion theory and engineering from the Nanjing University of Aeronautics and Astronautics (NUAA), Nanjing, China, in 1987 and 1998, respectively.

From 1996 to 1997, he was a as a Visiting Scholar with the University of Texas, Austin, TX, USA. He is currently a Professor with the College of Energy and Power Engineering, NUAA. His research interests include methods of modeling and control for aircraft engines.



Binbin Gu received the B.S. and M.S. degrees in flight vehicle power engineering and aerospace propulsion theory and engineering from the Nanjing University of Aeronautics and Astronautics, Nanjing, China, in 2015 and 2018, respectively.

He is currently a Principal Engineer with the Aero Engine Control System Institute, Wuxi, China. His research interests include controller design and the engineering applications for aircraft engines.



Ye-Hwa Chen received the Ph.D. degree in mechanical engineering from the University of California, Berkeley, CA, USA, in 1985.

He is currently a Professor with the Georgia Institute of Technology, Atlanta, GA, USA. His research interests include advanced control methods, neural networks and fuzzy engineering, adaptive robust control of uncertain systems, and uncertainty management.

Dr. Chen is a Member of the American Society of Mechanical Engineers and Sigma Xi. He is also a Regional Editor (North America) of *Nonlinear Dynamics and System Theory* and an Associate Editor of the *International Journal of Intelligent Automation and Soft Computing*.